2010

Computational and Thermodynamic Investigation of Condensing Injector Theory and Applications

Thomas W. Furlong
University Of Massachusetts

Michael F. Colarossi
University Of Massachusetts

Mark J. Bergander
Magnetic Development

David P. Schmidt
University of Massachusetts Amherst

Computational and Thermodynamic Investigation of Condensing Injector Theory and Applications

Thomas W. FURLONG[2], Michael COLAROSSI[2],
Mark J. BERGANDER[1]*, David P. SCHMIDT[2]

[1]Magnetic Development, Inc.
Madison, CT, USA, Ph.: 203-421-3562, E-mail: mark@mdienergy.com

[2]University of Massachusetts
Amherst, MA, USA, Ph.: 413-545-1393, E-mail: schmidt@ecs.umass.edu

* Corresponding Author

ABSTRACT

Widespread research of single phase injectors has led to the development of more efficient refrigeration cycles that utilize the pressure rise induced by injectors without the input of work. The current work presented here focuses on the application of a two-phase condensing injector in a refrigeration cycle to produce a more efficient cycle. A thermodynamic investigation shows the application and limitations of a condensing injector in a two loop refrigeration cycle. The flow through a condensing injector is modeled using semi-empirical method based on an Eulerian pseudo-fluid approach using a modified form of the Homogenous Relaxation Model (HRM) implemented within the framework of OpenFOAM. The predictions are found to be metastable, in that a solution is highly dependent on inlet conditions.

1. INTRODUCTION

An injector is a device intended to increase the pressure of a flow without the input of work (Trela et al., 2008). It is often interchangeably called an ejector, which is an equivalent device, but with the intended purpose of creating suction from a reservoir. In general, an injector can be described by the five basic components shown in Figure 1 (Chunnanond and Aphornratana, 2004), where location P is where the primary fluid enters the injector and S is the entrance for the secondary fluid. The primary nozzle inlet, section P to ii, is composed of a de Laval nozzle (converging-diverging) that is used to accelerate and expand the high pressure flow of the primary, or motive, stream into the mixing chamber. The mixing chamber, section ii to iv, is the location of mixing between the primary and secondary streams. The constant area section, section iv to vi, is a region of constant area with flow through a pipe. The diffuser, section vi to vii, decreases the velocity of the flow in order to convert the kinetic energy into an increase in pressure at the outlet of the injector.

Injectors can be divided into two classifications based upon the geometrical location of the primary nozzle inlet. The first is the constant area mixing injector, or constant area injector, which places the outlet of the primary nozzle inlet within the constant area section of the injector. Under these conditions, the mixing chamber and the constant area sections are equivalent. The second is the constant pressure mixing injector, or constant pressure injector, which places the outlet to the primary nozzle inlet within the mixing chamber and a known distance from the constant area section. Past research on injectors has been focused on single phase constant pressure injectors, where the working fluid is vapor at both the primary and secondary inlet (Chunnanond and Aphornratana, 2004). This work will focus on two-phase constant area injectors, where the working fluid is liquid at the primary inlet and vapor at the secondary inlet, in order to have comparable two-phase experiments.

2. TWO PHASE INJECTOR THEORY

A two phase injector utilizes the sub-cooled liquid and vapor phases of a single working fluid as the primary and secondary flow inlets. The large temperature differences between the primary and secondary flow, coupled with the high relative velocity establishes a high rate of heat transfer (Levy and Brown, 1972).

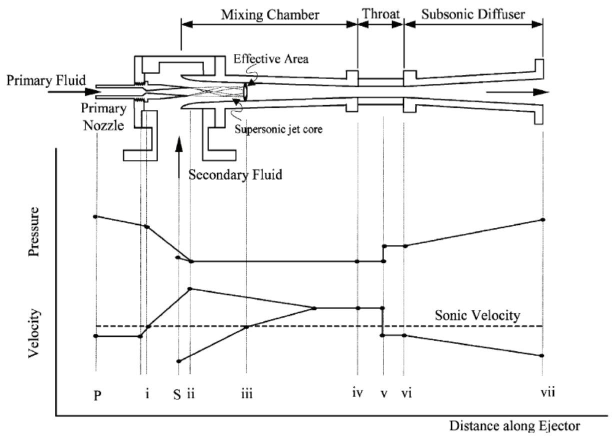

Figure 1: Basic Elements of a Constant Pressure Injector (Chunnanond and Aphornratana, 2004)

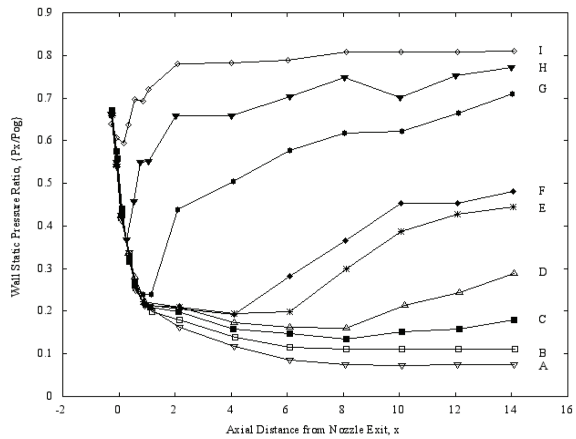

Figure 2: Effect of Inlet Liquid Velocity on Axial Wall Static Pressure in a Constant Area Injector (BPVO) (Levy and Brown, 1972)

Under the proper inlet conditions, the mixing of the primary and secondary flows causes a condensation shock to occur, where the two-phase flow condenses into liquid over a short distance (Levy and Brown, 1972). For this reason, two phase injectors are commonly referred to as condensing injectors (CI). Levy (1967) also showed that the condensation shock can cause a pressure rise across the injector, where the outlet pressure is greater than the primary and secondary inlet pressures.

Experiments conducted by Levy and Brown (1972) for a constant area CI determined the criteria for a condensation shock to occur. It was found that a condensation shock could not occur with the Back Pressure Valve Open (BPVO), regardless of the inlet conditions, due to the liquid stream creating a cylindrical jet in the center and the vapor creating an annular region at the wall with little to no mixing occurring. As the Back Pressure Valve was Closed (BPVC), a condensation shock occurred under proper inlet conditions due to the mixing of the primary and secondary flows. In order to gain insight into other factors effecting condensation shock, further experiments were conducted with the BPVO. With the BPVO, the flow of the constant area CI can be divided into three distinct regimes, shown in Figure 2 (Levy and Brown, 1972). Regime I, given by runs A, B, C, and D, is termed the High Inlet Liquid Velocity Flow Regime. Within this regime the liquid jet keeps a defined cylindrical jet until approximately x=5 (varies from x=5 to x=9), where the liquid jet breaks up resulting in a two-phase cylindrical jet region with a supersonic annular vapor phase region. Regime II, given by runs E, F, G, and H, is termed the Intermediate Inlet Liquid Velocity Regime. Under these inlet conditions, the liquid jet breakup length was between x=1 and x=5 and the vapor Mach number dropped to a subsonic value at approximately x=3. Regime III, given by run I, is termed the Low Inlet Liquid Velocity Regime. In this region the liquid jet breakup is just after the primary nozzle exit plane, where the Mach number of the vapor region is subsonic for the entirety of the injector. These regimes show that liquid jet breakup is accompanied by a sharp decrease in the vapor Mach number, resulting in a subsonic vapor region (Levy and Brown, 1972).

Based on the experiments conducted by Levy and Brown (1972), the following conditions must be satisfied for a condensation shock to occur. First the back pressure valve must be near BPVC conditions. Secondly, the inlet conditions of the flow must be in Regime I, as it is the only regime capable of producing a condensation shock. Regimes II and III do not produce a condensation shock due to early liquid jet breakup that causes the vapor Mach number to become subsonic. And lastly, a necessary, but not sufficient condition is supersonic vapor flow because increases in wall static pressure due to the closing of the back pressure valve begin within the supersonic vapor flow.

3. CONDENSING INJECTOR REFRIGERATION CYCLE

A typical refrigeration cycle is composed of an evaporator, a condenser, a compressor, and an expansion valve. The expansion valve throttles the working fluid to a lower, more desirable pressure in order for evaporation to occur at a lower temperature. The isenthalpic throttling process dissipates kinetic energy that could be recovered by using an injector. As previously determined, an injector has the ability to induce a pressure rise across the injector. By placing the injector in a refrigeration cycle, less work is required by the compressor resulting an increased efficiency. A single phase injector was inserted into a refrigeration cycle created by Kornhauser (1990) and produced a theoretical improvement of 21% and an experimental improvement of 5%. Using the same cycle with transcritical CO_2, Li and Groll (2005) were able to achieve a 16% increase in the Coefficient of Performance (COP).

Recently, a refrigeration cycle involving the use of a two phase condensing injector has been studied that takes flow from the outlet of the condenser and sends it to the injector to produce a second stage of compression (Bergander, 2006). Figure 3 shows the CI refrigeration cycle where A is the evaporator, B is the compressor, C is the injector, D is the condenser, E is the separator, F is the expansion valve, and G is the pump. Early thermodynamic models showed that this cycle, with R-22 as the working fluid, is capable of improving the COP over a typical refrigeration cycle by 38% and an initial experimental result showed 16% improvement (Bergander, 2006).

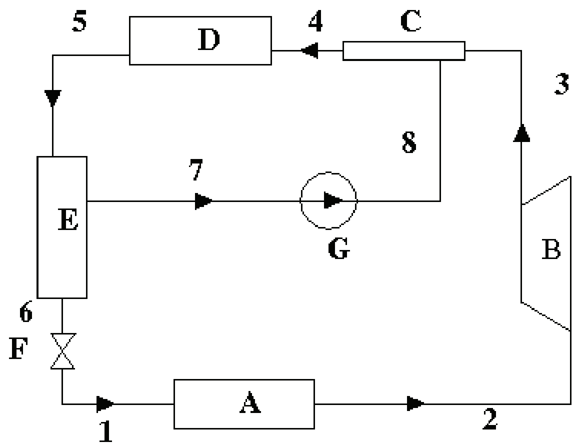

Figure 3: Condensing Injector Refrigeration Cycle

It had been suggested that the pressure at the outlet of the injector would be capable of being greater than both of the inlets (Bergander, 2006). While theory and experiments by Levy (1967) have previously shown a pressure rise is possible for an injector, an unstable loop could be created by the pressure rise when inserted into a cycle. The change in pressure of each loop has to equal such as in the secondary loop, given by 5-7-8-4.. In order to stabilize the cycle, several assumptions must be made. The injector is first assumed to be adiabatic. Secondly it is assumed that no work is done by or on the injector. To limit the pressure rise across an injector, it is assumed that the pressures at the primary inlet, p_8, and the outlet, p_4, are equal, consistent with the assumption that any pressure rise associated with the pump, G, is balanced by losses in the condenser, D.

The control volume approach can be utilized about the injector to find the relation given in Equation (1). Equation (1) represents the pressure change across the injector due to the change in internal energy plus the change in kinetic energy.

$$\frac{(1+\omega)p_4}{\rho_4} - \frac{\omega p_3}{\rho_3} - \frac{p_8}{\rho_8} = -(1+\omega)u_4 + \omega u_3 + u_8 + \frac{1}{2}\left(-(1+\omega)V_4^2 + \omega V_3^2 + V_8^2\right) \qquad (1)$$

Where p, u, V, ω, and ρ are the pressure, internal energy, velocity, entrainment ratio, and the density respectively. In order to analyze Equation (1), the Engineering Equation Solver (EES) was utilized to solve the equations of the cycle based on conditions stipulated in Table 1 and using R-22 as the working fluid, where 1 to 2 is isobaric vaporization, 2 to 3 is isentropic compression, 3/8 to 4 is the injector process, 4 to 5 is non-isobaric condensation, 5 to 6/7 is separation, 7 to 8 is isentropic compression, and 6 to 1 is isenthalpic expansion.

From the assumption that $p_8=p_4$, it can be approximated that $\rho_8=\rho_4$ and Equation (1) can be reduced to Equation (2):

$$\frac{\omega p_4}{\rho_4} - \frac{\omega p_3}{\rho_3} = -(1+\omega)u_4 + \omega u_3 + u_8 + \frac{1}{2}\left(-(1+\omega)V_4^2 + \omega V_3^2 + V_8^2\right) \qquad (2)$$

Table 1: Refrigeration Cycle Requirements

Position	p (kPa)	T (C)	*h* (kJ/kg)	*s* (kJ/kg K)	x
1	421.3	-	h_6	-	-
2	p_1	-5	-	-	-
3	1190	-	-	s_2	-
4	p_8	-	-	-	0.01
5	p_4-550	-	-	-	0
6	p_5	-	-	-	0
7	p_5	-	-	-	0
8	p_7+550	-	-	s_7	-

Based on the values in Table 1, the secondary inlet values are p_3=1190 kPa and $\rho_3 \approx 45$ kg/m^3. The primary inlet and outlet values, which have been assumed to have equal pressures, have to be greater than the secondary inlet to utilize the benefits of the condensing injector. Therefore the pressure and density for the outlet, position 4, can be determined for pressures greater than 1190 kPa, where the density is assumed to be given by its saturation properties. For all pressures less than 15600 kPa at the outlet, the left hand side of Equation (2) will be negative. A pressure rise greater than 15600 kPa is not feasible and therefore the left hand side of Equation (2) must be negative. While this analysis is for a specific case, it should be noted that the analysis can be confidently applied to many cases as the assumptions of the analysis remain the same. Also note that the assumptions that $\rho_8=\rho_4$ and that ρ_4 is given by the saturation point are very approximate, but they allow this analysis to proceed in a manner that produces accurate results due to the values keeping the same trends within the flow.

From the knowledge that the left hand side of Equation (2) is negative, it can then be inferred that the right hand side must also be negative. It is known from the cycle analysis in EES that the change in internal energy across the injector is more negative than the pressure change; therefore the change in kinetic energy across the injector must be positive in order to satisfy Equation (2) resulting in a relation given by Equation (3).

$$\frac{1}{2}\left(-(1+\omega)V_4^2+\omega V_3^2+V_8^2\right)>0 \tag{3}$$

The relation given by Equation (3) shows that the velocity at the outlet, position 4, will be small relative to the two inlets, indicating that the kinetic energy is dissipated in the injector. This follows with the theory of a diffuser, which can be considered a much simpler injector, where the kinetic energy is reduced in order to get a pressure increase. This analysis shows that the assumption that a pressure rise can occur across an injector are thermodynamically valid. It also shows that p_4 can not be thermodynamically restricted to equal p_8 and the injector and cycle must be designed to induce this.

4. MODELING APPROACH

The condensing injector flow is modeled using the pseudo-fluid approach, where the transport equations of conservation of mass, momentum, and enthalpy, Equations (4), (5), and (6) respectively, are utilized to treat the two phases as a single fluid.

$$\frac{\partial \rho}{\partial t}+\nabla\phi=0 \tag{4}$$

$$\frac{\partial \rho V}{\partial t}+\nabla(\phi V)=-\nabla p+\nabla\vec{\vec{\tau}} \tag{5}$$

$$\frac{\partial \rho h}{\partial t}+\nabla(\phi h)-\nabla\left(\frac{\mu}{\mathrm{Pr}}\nabla h\right)=\frac{\partial p}{\partial t}+\vec{V}\cdot\nabla p \tag{6}$$

Where h, Pr, t, μ, τ, and ϕ are the enthalpy, Prandtl number, time, viscosity, stress tensor, and the mass flux respectively. In the numerical simulation, as each conservation equation is solved, thermodynamic properties need to be updated. The fluid properties are obtained using Reference Fluid Thermodynamic and Transport Properties Database (REFPROP) from the National Institute of Standards and Technology (NIST) database. REFPROP is utilized to create a data table based on two thermodynamic properties input by the user over a specified range and step size. For this work, a table based on pressure and enthalpy points is input into REFPROP, where it calls the subroutines necessary to provide the requested thermodynamic outputs.

In order to close the system described by the conservation Equations (4), (5), and (6) an equation of state would normally be applied. However, under the conditions of two-phase flow there is no direct method to calculate an appropriate equation due to the mixing and heat transfer between the phases during condensation. Another complication is that the two-phase mixture is not in thermodynamic equilibrium. A modified form of the Homogenous Relaxation Model (HRM) is utilized to bring the mixture towards equilibrium. HRM is based on a linear expansion of the quality over a timescale, shown in Equation (7), proposed by Bilicki and Kestin (1990).

$$\frac{Dx}{Dt} = \frac{\bar{x} - x}{\Theta} \tag{7}$$

Where x and $\bar{x}$ are the mass vapor fraction and the equilibrium mass vapor fraction respectively and the timescale, Θ, for the HRM is found by inserting the best fit values from experiments conducted by Downar-Zapolski et al. (1996) into Equation (8).

$$\Theta = \Theta_0 \alpha^a \psi^b \tag{8}$$

Where the constants Θ_0, a, and b are the best fit values equal to $6.51 \cdot 10^{-4}$ [s], -0.257, and -2.24 respectively. The variable α is the vapor volume fraction and ψ is a dimensionless pressure difference given by Equation (9).

$$\psi = \left| \frac{p_{sat} - p}{p_{sat}} \right| \tag{9}$$

For an incompressible variable density flow, the divergence of the velocity field is non-zero. The total derivative of density can be expanded into Equation (10) to determine the divergence of velocity.

$$\frac{D\rho}{Dt} = \left.\frac{\partial\rho}{\partial p}\right|_{x,h} \frac{Dp}{Dt} + \left.\frac{\partial\rho}{\partial x}\right|_{p,h} \frac{Dx}{Dt} + \left.\frac{\partial\rho}{\partial h}\right|_{p,x} \frac{Dh}{Dt} \tag{10}$$

Equation (10) splits the density change into contributions of Mach effects, variations due to concentration differences, and thermal expansion effects, where Mach effects and thermal expansion contributions are assumed negligible. The divergence of the velocity field is then described by Equation (11).

$$\nabla \cdot V = -\frac{1}{\rho} \left.\frac{\partial\rho}{\partial x}\right|_{p,h} \frac{Dx}{Dt} \tag{11}$$

The momentum equation can be generalized into Equation (12), where a_p is the diagonal coefficient of the momentum equation matrix and H(V) is the off-diagonal terms caused by convection and diffusion with neighboring cells.

$$a_p U_p = H(V) - \nabla p \tag{12}$$

The divergence of Equation (12), combined with Equation (11) results in Equation (13).

$$\rho\nabla \cdot \left(\frac{H}{a_p}\right) - \rho\nabla \frac{1}{a_p} \nabla p + \left.\frac{\partial\rho}{\partial x}\right|_{p,h} \frac{Dx}{Dt} = 0 \tag{13}$$

To extend the validity of the classic HRM method for flash boiling to use in condensation changes were made to the defining equations. Turbulent mixing terms have been introduced into the transport equations for quality, momentum, and enthalpy in order to achieve the degree of mixing that is experimentally observed. A similar pseudo-fluid Eulerian framework has previously been utilized to predict the turbulent atomization of a liquid jet using the turbulent mixing terms in the Σ-Y model (Trask et al., 2010). This turbulent mixing approach assumes the scales at which turbulent mixing occurs are separate from those of the bulk fluid motion at high Reynolds and

Weber numbers. This allows the turbulent mixing and generation of interfacial surface area to be resolved through classical turbulence the closures using the k-epsilon model (Launder et al., 1975) for Reynolds stresses and a turbulent diffusion hypothesis for the characterization of turbulent mixing of liquid and vapor.

To accommodate the process of condensation, an extra term was added to Equation (8) provide symmetry of phases. The timescale was bounded above and below to avoid numerical instability. The open source OpenFOAM framework is utilized to provide the structure for solving the set of equations in an object-oriented framework (Weller et al., 1998). Solvers written with OpenFOAM are capable of decomposed parallel cases using a message passage interface (MPI) and are compatible with fully three-dimensional general polyhedral meshes. A numerical approach that incorporates the HRM model can be seen in Schmidt et. al, (2009) and the numerical approach with the Σ-Y model included with the HRM model can be seen in Colarossi et. al (2010).

5. LEVY-BROWN CONDENSING INJECTOR

The condensing injector to be modeled is based on the experimental work conducted by Levy and Brown (1972). The two-dimensional flow is axisymmetric about the centerline axis. Under the conditions simulated, saturated vapor enters through the annular channel and saturated liquid enters axially.

The velocity at the gas inlet is set to Mach 1 and the velocity at the liquid inlet is set to 30 m/s, which are similar values to those used by Levy and Brown (1972). The outlet boundary condition on the velocity gradient is set to zero. Fixed uniform densities of 0.59 kg/m3 at the gas inlet and 997.1 kg/m3 at the liquid inlet are imposed. Zero pressure gradient boundary conditions are specified at the inlets. At the outlet, a non-reflecting boundary condition of 4 bar is imposed. All walls are adiabatic.

6. RESULTS

This simulation presented here was run for 0.075 seconds of simulated time, and the flow was able to reach steady state. Figure 4 shows that there is mixing between the vapor and liquid streams, and that by the nozzle exit the flow is mostly liquid, but has not completely condensed. This mixing is caused by the high enthalpy of the gas mixing with the low enthalpy of the liquid. This mixing predisposes the vapor to condense by lowering its temperature. Around the centerline the mass fraction of vapor is very close to zero, while along the top wall of the vapor stream area the mass fraction of vapor is close to 0.02.

Figure 5 shows the pressure distribution through the nozzle. Though the trend does look similar to what is seen in Figure 1, the pressure at the outlet does not have a significant increase compared to the inlet pressure. This is because there is no condensation shock seen in the simulation. Also, from the turbulence model, it predicts a higher pressure at the gas inlet and a lower pressure at the liquid inlet (as compared to the turbulence effects not being included).

7. CONCLUSIONS

The condensing injector has been thermodynamically shown to be an effective way to increase the efficiency of a refrigeration cycle. The analysis also showed that the pressure at the exit of the condensing injection cannot be greater than both of the inlets due to the stability of the refrigeration cycle. However, an increase in efficiency can still occur by raising the pressure of the secondary inlet flow to that of the primary inlet flow.

The idea embodied in the Homogenous Relaxation Model was used to construct a CFD model for a condensing injector. Though further model adjustment and experimental validation is required, it is an encouraging early result. The current implementation benefits from the flexibility of the OpenFOAM libraries.

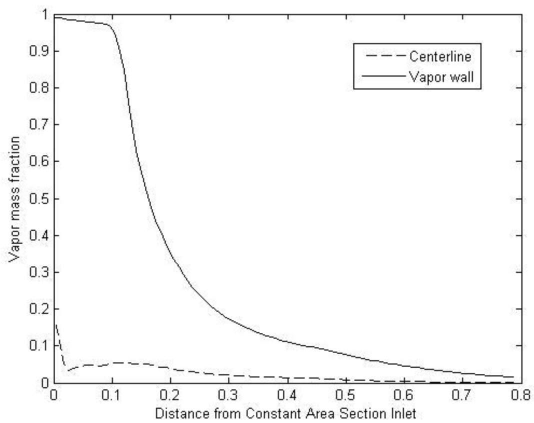

Figure 4: Vapor Mass Fraction Across CI

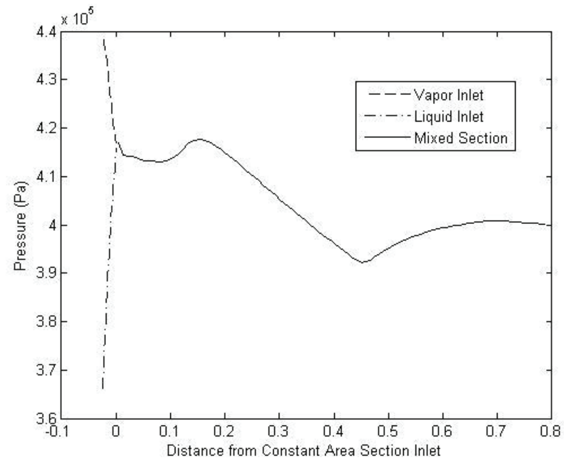

Figure 5: Pressure Distribution Through CI

The preliminary numerical results show condensation occurring through the nozzle, but do not show the expected shock leading to rapid condensation. The expected pressure rise is not seen in the simulation because of the lack of a condensation shock.

Continuing work will use experimental validation to adjust the model to improve its accuracy and check the general applicability of the model's ability to predict condensation. While the current approach to model the effects of turbulence are successful in predicting the mixing process between the two phases, additional investigation of the appropriate boundary conditions is required to better match the experimental behavior of the injector.

8. ACKNOWLEDGEMENTS

This material is based upon work supported by the National Science Foundation, STTR Phase II Project No. 0822525 and by the Department of Energy, under Award Number DE-FG36-06GO16049

9. DISCLAIMER

REFERENCES

Bilicki Z., Kestin J., 1990. Physical Aspects of the Relaxation Model in Two-Phase Flow. Proc. Roy. Soc. London A. 428, 379-397

Chunnanond, K., Aphornratana, S., 2004. Ejectors: Applications in Refrigeration Technology. Renewable and Sustainable Energy Reviews 8, 2, 129-155.

Colarossi M., Trask N., Schmidt D.P., Bergander M.J., 2010. Multidimensional Modeling of Condensing Two-Phase Ejector Flow. Submitted to International Journal of Refrigeration.

Downar-Zapolski P., Bilicki Z., Bolle L., Franco J., 1996. The Non-Equilibrium Relaxation Model for One-Dimensional Flashing Liquid Flow. IJMF 22, 3, 473-483.

Huang B.J., Change J.M., Wang C.P., Patrenko V.A., 1999. A 1-D Analysis of Ejector Performance. Int. J. Refrigeration, 22, 5, 354-364.

Keenan H., Neumann E.P., Lustwerk F., 1950. An Investigation of Ejector Design by Analysis and Experiment. J. Appl. Mech. ASME 17, 3, 299-309.

Launder B.E., Reece G.J., Rodi W., 1975. Progress in the Development of a Reynolds-Stress Turbulence Closure. Journal of Fluid Mechanics 68, 3, 537-566.

Levy E.K., Brown G.A., 1972. Liquid-Vapor Interactions in a Constant-Area Condensing Ejector. Journal of Basic Engineering 94, 1, 169-180.

Li D., Groll E.A., 2005. Transcritical CO_2 Refrigeration Cycle with Ejector-Expansion Device. Int. J. Refrigeration 28, 5, 766-773.

Munday J.T., Bagster D.F., 1977. A New Theory Applied to Steam Jet Refrigeration. Ind. Eng. Chem. Process Des. Dev. 16, 4, 442-449

Schmidt D.P., Gopalakrishnan S., Jasak H., 2009. Multi-dimensional simulation of thermal non-equilibrium channel flow. Int. J. Multiphase Flow.

Trela, M., Kwidzinski R., Butrymowicz D., 2008. Exergy analysis of losses in a two-phase steam-water injector. Chemical and Process Engineering 29, 2, 452-464.

Weller H.G. Tabor G., Jasak H., Fureby C., 1998. A Tensorial Approach to Computational Continuum Mechanics Using Object-Oriented Techniques. Computers in Physics 12, 6, 620.

Bergander, M.J., 2006. Refrigeration Cycle with Two-Phase Condensing Ejector. *Intern. Refrigeration and Air Conditioning Conf. at Purdue*, July 17-20, Paper No. R008.

Kornhauser, A.A., 1990. The use of an Ejector as a Refrigerant Expander. *Proc. of USNCR/IIR-Purdue Refrigeration Conference*, West Lafayette, IN. p. 10-19.

Trask N., Perot J.B., Schmidt D.P., Meyer T., Lightfoot M., Danczyk S., 2010. Modeling of the Internal Two-Phase Flow in a Gas-Centered Swirl Coaxial Fuel Injector. *48th AIAA Aerospace Sciences Meeting*.

Levy, E., 1967. Investigation of liquid-vapor interactions in a constant area condensing ejector. SCD Thesis, Dept. of Mech. Eng., MIT, Cambridge, Mass.